Available online at www.sciencedirect.com
SCIENCE DIRECT
Polymer 46 (2005) 4670–4675
polymer
www.elsevier.com/locate/polymer

# ATR–FTIR and NMR spectroscopic studies on the structure of polymeric gel electrolytes for biomedical applications

Silvia Licoccia[a,*], Marcella Trombetta[b], Donatella Capitani[c], Noemi Proietti[c], Paola Romagnoli[b], M. Luisa Di Vona[a]

[a]*Department of Chemical Science and Technology, University of Rome 'Tor Vergata', Via della Ricerca Scientifica 1, 00133 Rome, Italy*
[b]*Laboratory of Biomaterials, Interdisciplinary Center for Biomedical Research (CIR), University 'Campus Bio-Medico', via E. Longoni 83, 00155 Rome, Italy*
[c]*Institute of Chemical Methodologies, CNR, Research Area of Rome M.B.10, 00016 Monterotondo Stazione, Rome, Italy*

Received 30 June 2004; received in revised form 4 February 2005; accepted 22 March 2005
Available online 22 April 2005

**Abstract**

The structure of polymeric gel membranes to be used as electrolytes in the recording of bioelectrical signals has been investigated by means of ATR–FTIR and $^{7}$Li and $^{13}$C MAS NMR spectroscopies. The membranes, based on PMMA, 1,2-diethoxyethane and lithium perchlorate, showed different ionic conductivity as a function of their composition. Such differences have been analyzed on the basis of spectroscopic data and the existence of interactions with the ester function in the polymeric matrix was determined. Spectroscopic data allowed to establish the optimal lithium concentration needed to achieve best ionic conductivity.


*Keywords:* PMMA; ATR–FTIR; NMR

## 1. Introduction

The peculiar properties of polymer gels has made them the subject of numerous studies, their applications ranging from tissue engineering to electrochemistry [1]. In the field of bio-materials polymeric gels were used in fact for encapsulating living cells and, more recently, as matrixes for regenerating and repairing a wide number of living tissues and organs [2–5]. The incorporation of Li salts and non-aqueous solvents into a polymeric matrix led to the development of gel type electrolytes characterized by a high ionic conductivity, comparable to that of liquid electrolytes [6]. Because of their unique network structure, gels always posses simultaneously both the cohesive properties of solids and the diffusive transport properties of liquids. Thus polymeric gels electrolytes have been used in a variety of electrochemical devices such as lithium-ion batteries, supercapacitors, electrochromic windows, and sensors [7–11]. Among the various polymers studied, a great deal of investigations have been devoted to poly(methylmethacrylate) (PMMA). Its use as gelatinization agent in an electrolyte was first announced by Ijima et al. in 1985 [9,12]. They reported that a conductivity of $10^{-3}$S cm$^{-1}$ at 25 °C was obtained with 15 wt% PMMA and later, Bohnke et al. dissolved PMMA in $LiClO_4$(1 M)-PC electrolyte at room temperature to achieve a homogeneous and transparent gel [13]. The high affinity for plasticizing organic solvents and lithium ions of PMMA are attributed to the presence of a polar functional group and its ion-transport mechanism is known to be more complex than that described by a model of connected liquid electrolyte regions in an inert polymeric matrix [9].

Coupling biocompatibility and electrochemical properties led us to develop new PMMA based ion conducting membranes to be used as interface between the skin and electrical instrumentation to produce an electroencephalogram (EEG), to register bioelectrical signals in extreme conditions. This work is in fact part of an interdisciplinary project called ALTEA (anomalous long term effects in astronauts) devoted to study the risk for functional brain anomalies due to cosmic rays during long space missions [14,15]. We previously reported on the preparation, electrochemical characterization and physico–chemical

* Corresponding author. Tel.: +39 672594386; fax: +39 672594328.
*E-mail address:* licoccia@uniroma2.it (S. Licoccia).

0032-3861/$ - see front matter © 2005 Elsevier Ltd. All rights reserved.
doi:10.1016/j.polymer.2005.03.078

Table 1
Composition and room temperature ionic conductivity of polymer gel electrolytes

| Label | [$Li^+$] (mol/l) | Conductivity (S $cm^{-1}$) |
|---|---|---|
| G1 | 0 | |
| G2 | 0.5 | $3.56\times10^{-4}$ |
| G3 | 0.8 | $1.63\times10^{-3}$ |
| G4 | 1.0 | $1.51\times10^{-3}$ |
| G5 | 1.5 | $4.46\times10^{-4}$ |

and electrical stability of new ionoconducting membranes that were successfully used to register EEG signals almost identical to those measured simultaneously with a conventional apparatus [15].

Properties of ionoconducting polymeric materials are known to depend on chemical structure and composition of monomer units, on the primary and higher order structure, on interactions between polymer chains and solvents, salts and so on. We have now studied by means of ATR/FTIR and MAS NMR spectroscopies the ionic interactions, environment and mobility in the PMMA/1,2-dietoxyethane/$LiClO_4$ based gel electrolytes developed for the specific biomedical application. The effect of salt concentration has been considered and a correlation has been sought between ion association and molar conductivity. FTIR and NMR have been chosen as investigating tools because they are among the most powerful means for studying the structure and dynamic of polymer gel systems. High resolution solid-state NMR is a non-invasive method that provides information on microscopic chemical structure trough the study of chemical shifts, signal splitting, shapes and molecular motion through relaxation rates. Although ionic conductivities of gels approach those of liquid electrolytes above ambient temperature, previous NMR results indicate that the immediate environments of both cations and anions differ significantly in the gel and in the liquid because the line-width for $^7Li$ spectra are distinctly larger for solid membranes [16]. The smaller line widths for the liquid reflect the efficient averaging of the dipolar interaction due to rapid lithium ion motion. Moreover the microscopic environment surrounding $Li^+$ ions are largely uniform without significant phase separation between polymer and liquid component [16,17]. Vibrational spectra provide information through frequencies, intensities and other band properties which can be used to identify species and chemical processes, spectral studies can help to identify factors that affect the general properties and performance of the electrolyte system [18,19].

## 2. Experimental

### 2.1. Materials

All products (Aldrich) were reagent grade and were used as received. The electrolyte membranes were prepared by immobilizing solutions $LiClO_4$ in 1,2-diethoxyethane in a poly(methylmethacrylate) (PMMA, MW 996000) matrix. All the gels were prepared by the solvent casting technique. The details of the procedure were reported in previous work [15]. Transparent films with an average thickness of 0.5–1 mm were obtained. The molar ratio between 1,2-diethoxyethane and PMMA was kept constant at 2.6 while the concentration of $LiClO_4$ was varied from 0 to 1.5 M. The membranes were labeled G1–G5 and their different compositions are listed in Table 1 together with conductivity values.

### 2.2. Measurement

#### 2.2.1. Conductivity

Ionic conductivity was measured at room temperature by impedance spectroscopy performed on Teflon cells formed by sandwiching the given membranes between two stainless steel electrodes. The measurements were carried out using a Solartron frequency response analyzer (model 1260) scanning over 1 Hz–100 kHz.

#### 2.2.2. NMR

$^7Li$ MAS NMR spectra were measured on a Bruker AMX-200 spectrometer operating at 77.78 MHz. Samples were introduced into 4 mm Zirconia rotors and sealed with Kelf caps. The spin rate was kept at 3 kHz. The $\pi/2$ pulse width was 9 μs, the recycle time was 3 s. LiCl (aq) solution (0 ppm) was used as external reference for chemical shifts. $^{13}C$ single pulse excitation (SPE) spectra were recorded at 50.13 MHz, the recycle time was 3 s, the $^{13}C$ $\pi/2$ pulse was 4 μs. Spectra were obtained using 2048 data points in the time domain, zero filled and Fourier transformed to a size of 4096 data points. The $^{13}C$ chemical shifts were externally referred to tetramethylsilane. All the spectra were recorded at the probe temperature ($\approx$293 K).

Deconvolution of $^7Li$ NMR spectra was carried out with the SHAPE 2000 (version 2.1) software package developed by Prof Michele Vacatello, Naples University, Italy.

$T_1$ spin lattice relaxation times were measured applying the Inversion Recovery pulse sequence (180°–$\tau$–90°). The values were obtained from exponential fits to the signal intensities measured in spectra run with different relaxation delays.

#### 2.2.3. FTIR

ATR/FTIR analysis was performed using golden gate MK II single reflection diamond ATR systems, Specac mounted on a spectrophotometer FTIR Nexus 870 ESP, Nicolet. Membranes samples were analyzed directly on an ATR platform.

## 3. Results and discussion

The gelation mechanism of PMMA in different solvents

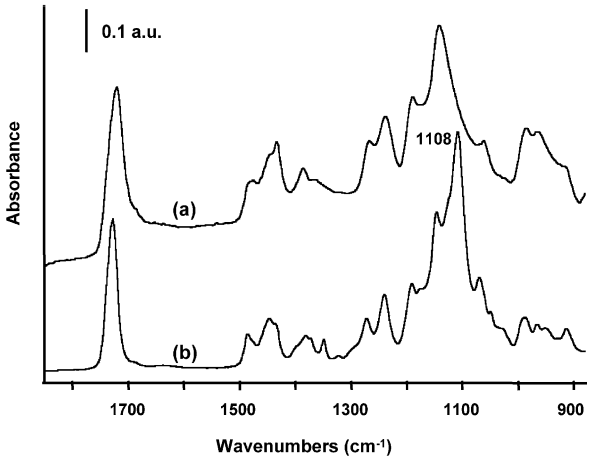


Fig. 1. ATR–FTIR spectra of (a) pure PMMA, (b) PMMA based membrane G1.

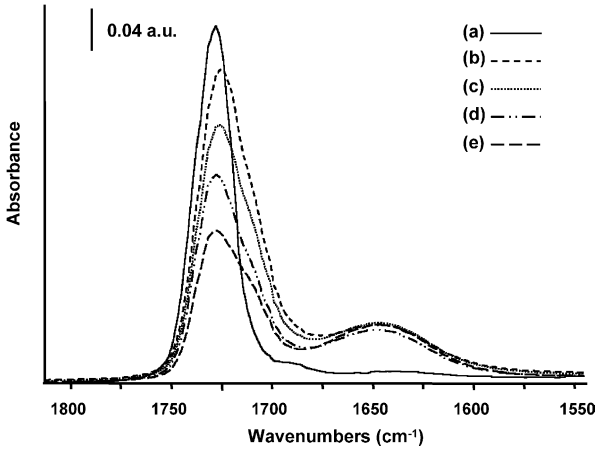


Fig. 3. ATR–FITR spectra of the $\nu$C=O region of PMMA based membranes (a) G1; (b) G2, $[Li^+]=0.5$ M; (c) G3, $[Li^+]=0.8$ M; (d) G4, $[Li^+]=1.0$ M; (e) G5, $[Li^+]=1.5$ M. Labels refer to Table 1.

has been previously investigated by different authors [18–20]. To characterize the process occurring in 1,2-diethoxyethane we measured the ATR/FTIR spectra of PMMA before and after gelation. Fig. 1 shows the spectral region 1850–850 $cm^{-1}$, where no IR active bands due to 1,2-diethoxyethane are present. The spectrum of pure PMMA corresponds to that reported in the literature [21] with characteristic bands at 1720 $cm^{-1}$ ($\nu$C=O), 1440 $cm^{-1}$ ($\nu$O–$CH_3$) and the four bands due to vibrations of the ester group at 1270–1140 $cm^{-1}$ ($\nu_{AS}$C–C–O+$\nu_S$C–O). Upon gel formation, the intensity of the band due to $\delta$O–$CH_3$ (1440 $cm^{-1}$) decreases and the band due to $\nu$C=O shifts from 1720 to 1728 $cm^{-1}$. However, the main difference that can be observed in the spectrum of the gel is the appearance of a new intense band at 1108 $cm^{-1}$ (Fig. 1(b)). A similar absorption (1104 $cm^{-1}$) was observed for a gel obtained in 2-butanone and was attributed to a solvent assisted conformational change with the formation of a dimeric double helix structure [20]. These observation are in agreement with the occurring of electrostating interaction that lead to the formation of dimeric structures.

To obtain the required ionic conductivity $LiClO_4$ has then been added to the system. Fig. 2 shows the ATR/FTIR spectra of PMMA based gels with different lithium perchlorate concentration. Spectral features due to salt–polymer interactions are most evident in two spectral regions: 1800–1550 and 1300–1000 $cm^{-1}$. Some water was introduced in the sample with the highly hygroscopic lithium perchlorate as evidenced by the presence of the band at 1645 $cm^{-1}$ that can be observed in Fig. 3, which shows details of the spectral region characteristic of $\nu$C=O, and $\delta$OH. The intensity of the 1645 $cm^{-1}$ band is constant in the different samples and is independent from salt concentration. Also, in the spectral region characteristic of $\nu$O–H stretching (4000–3000 $cm^{-1}$, not shown), no significant variation in the number of bridged OH groups with salt concentration was observed. It follows that the number of electronegative substituents involved in hydrogen bonds

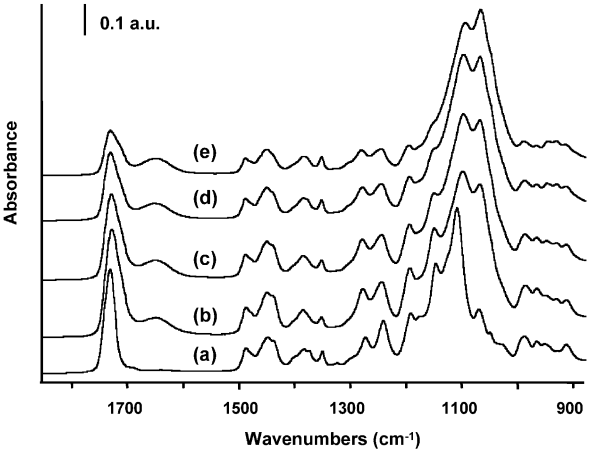


Fig. 2. ATR–FTIR spectra of PMMA based membranes. (a) G1; (b) G2, $[Li^+]=0.5$ M; (c) G3, $[Li^+]=0.8$ M; (d) G4, $[Li^+]=1.0$ M; (e) G5, $[Li^+]=1.5$ M. Labels refer to Table 1.

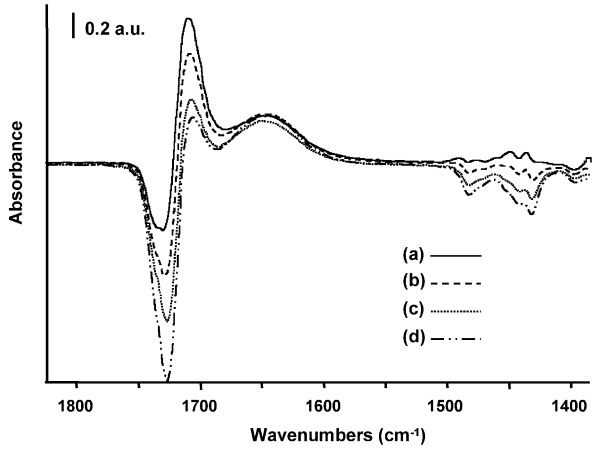


Fig. 4. Results of the subtraction (difference factor=1) of ATR–FTIR spectrum of sample G1 from those of samples (a) G2; (b) G3; (c) G4; (d) G5. Labels refer to Table 1.

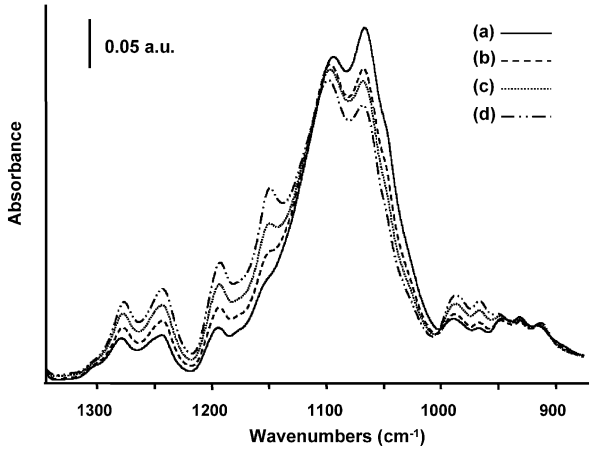


Fig. 5. ATR–FTIR spectra of the $\nu$Cl–O stretching region of PMMA based membranes. (a) G5, $[Li^+]=1.5$ M; (b) G4, $[Li^+]=1.0$ M; (c) G3, $[Li^+]=0.8$ M; (d) G2, $[Li^+]=0.5$ M. Labels refer to Table 1.

with water is independent from the amount of $LiClO_4$ introduced in the membrane, hence that the spectral variations that will be discussed are due to interactions with $Li^+$.

The spectra shown in Fig. 3 clearly show that increasing salt concentration results in modifications of the carbonyl band. To better analyze the spectral variations observed, difference spectra are shown in Fig. 4. The spectrum of the reference membrane, G1, was subtracted from those of the lithium containing samples with a subtraction factor equal 1. The $\nu$C=O region is characterized by a two components negative peak (1737 and 1728 $cm^{-1}$) which absolute intensity increases with salt concentration, and by a positive peak (1710 $cm^{-1}$) which shows opposite behavior. The presence of both peaks can be explained by the existence of electric dipole interactions between lithium ions and the polymer carbonyl groups. The two components (1737 and 1728 $cm^{-1}$) of the negative peak can be attributed to C=O groups involved in different interactions with $Li^+$, such as, for instance, the formation of a primary complex $Li^+\cdots$ O=C and a secondary complex between $Li^+$ and several carbonyl groups simultaneously [22]. Addition of $LiClO_4$ inhibits the IR activity of both components and this can only be due to the generation of novel interactions in the system. It should also be noticed in Fig. 4 that the 1440 $cm^{-1}$ band (assigned to $\nu$O–$CH_3$) is negative in the difference spectra and its absolute intensity increases with salt concentration.

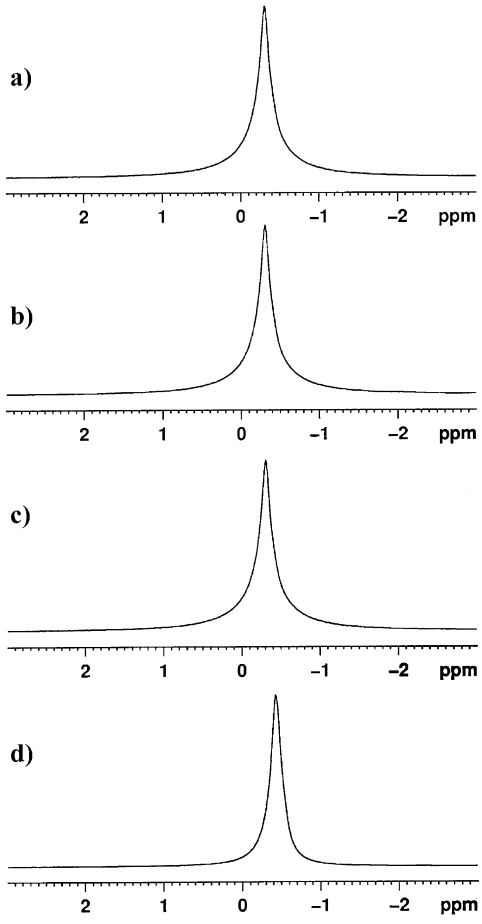


Fig. 6. $^7$Li MAS NMR spectra of membranes (a) G2; (b) G3; (c) G4; (d) G5. Labels refer to Table 1.

It is well known that electronegative groups, such as C=O and $OCH_3$ can interact with lithium ions [9]. The $Li^+\cdots$O=C interaction explains the decrease of the intensity of the original bands due C=O groups and the concomitant generation of the 1710 $cm^{-1}$ band. A decrease in intensity was also observed for the four bands due to PMMA in the region 1270–1140 $cm^{-1}$ (Fig. 5). These bands are due to the combination $\nu_{AS}$C–C–O + $\nu_S$C–O and their variation shows demonstrates the interaction with $Li^+$ of the whole ester group engaged in polymer chain mobility ($Li^+\cdots$O–$CH_3$).

The relative intensity of the 1710 $cm^{-1}$ band with respect to the higher energy C=O vibrations increases with $Li^+$ concentration. Its absolute intensity, however, decreases with increasing $[Li^+]$ and this can be explained assuming that some lithium is subtracted from the interaction with C=O groups by the formation of ion pairs. Fig. 5 shows the spectra of membranes G2–G5 in the region 1300–1000 $cm^{-1}$, where bands due to the perchlorate ion are expected. In the spectrum of pure $LiClO_4$ the $\nu$Cl–O band appears at 1093 $cm^{-1}$. The formation of $[Li^+ClO_4^-]$ ion pairs in the membranes is demonstrated by the presence of a new band at 1067 $cm^{-1}$; the intensity of both bands increasing with salt concentration. More interesting than the absolute intensity of these two bands is, however, their relative intensity, which can be correlated with conductivity data. Thus, for sample G2, $I_{1093}/I_{1067}>1$, but the number of cations present in the system is too low to achieve good conductivity. For sample G5 the ratio $I_{1093}/I_{1067}<1$ indicates that most $Li^+$ ions are involved in the formation of ion pairs in agreement with the low value of conductivity measured. Sample G3, for which $I_{1093}/I_{1067}$ is just higher than 1, represents the compositional limit to achieve good conductivity, as also shown by the decrease in

Table 2
NMR data for ionic conducting membranes Gn

| Label | $[Li^+]$ | $\delta^7$Li (ppm) | $^7$Li $\Delta\nu_{1/2}$ (Hz) | $^7$Li $T_1 \pm 10\%$ (ms) | $^{13}$C $\delta$C=O (ppm) | $^{13}$C $\Delta\nu_{1/2}$ (Hz) |
|---|---|---|---|---|---|---|
| G1 | 0 | | | | 177.9 | 118 |
| G2 | 0.5 | −0.31 | 23 | 171.8 | 178.9 | 259 |
| G3 | 0.8 | −0.31 | 20 | 219.2 | 179.6 | 259 |
| G4 | 1.0 | −0.37 | 18 | 170.4 | 179.9 | 140 |
| G5 | 1.5 | −0.43 | 14 | 196.4 | 179.9 | 140 |

electrical performance shown by membrane G4, where $I_{1093}/I_{1067} \approx 1$.

To further investigate the structural and dynamic properties of the systems we measured and analyzed the $^7$Li and $^{13}$C NMR spectra of the membranes.

Fig. 6 shows the MAS and proton decoupled $^7$Li NMR spectra obtained at room temperature for membranes G2–G5. Chemical shifts, line widths and spin–lattice relaxation times are reported in Table 2.

No substantial variation was observed both in chemical shifts and line width values, but the presence of two components (a narrow Lorenzian peak and a broad Gaussian one) was shown by fitting the data. Since the line width of a NMR signals is related to mobility, the narrow peak can be attributed to that fraction of Lithium ions responsible of conductivity, which occurs by fast ion transport, whereas the broad peak is due to the slow mobile ions [23]. Two inequivalent $Li^+$ sites appear then to be present, suggesting the existence of at least two different quadrupolar interactions and hence of two distinct $Li^+$ environments, most probably one where the ions are interacting with the polymer and the other in ionic clusters, in agreement with IR data.

Additional information regarding dynamic behavior can be obtained from $^7$Li spin–lattice relaxation times ($T_1$) measurements (Table 2). Although $T_1$ are very similar for all the membranes, the highest value was obtained for a salt concentration of 0.8 M, again in agreement with conductivity data. At the measurements temperature (293 K) the system is in the motionally narrowed region [18] and the decrease in $T_1$ indicates a decrease in mobility either of the lithium ion itself or of the local environment.

Fig. 7 shows the $^{13}$C MAS NMR spectrum of membrane G2, with assignment of individual resonances. The main difference with respect to the MAS NMR spectrum of the pure polymer are the small shifts observed for the resonances due to the C=O and $OCH_3$ groups from 177.6 (pure PMMA) to 177.3 ppm and from 51.6 to 52.6 ppm, respectively, indicating variations in the electron density on the C atoms in agreement with the coulombic interactions with lithium ions evidentiated by IR. The introduction of $LiClO_4$ causes only minor variation in the NMR spectra of the different membranes. Only small variations in the line shape or position of the resonances were observed for the different membranes. The largest effect was observed in the lineshape of the resonance due to the carbonyl group, which becomes narrower in the presence of lithium salt. Fig. 8 shows the spectra of membranes G2–G5 in the region 190–170 ppm. The observed line narrowing can be related to an increase in PMMA chain backbone mobility. The presence of different components of the C=O resonance maybe ascribed to the different interactions between $Li^+$ and the polymer, in agreement with IR data.

## 4. Conclusions

Analysis of the ATR–FTIR spectra of PMMA/1,2-diethoxyethane/$LiClO_4$ ionoconducting polymeric gel membranes allowed to establish the interactions occurring in the membranes. The existence of $Li^+\cdots O{=}C$ and $Li^+\cdots O{-}CH_3$ interactions was demonstrated to be competitive with the formation of ion pairs. The anion spectral features allowed to establish the optimal concentration of

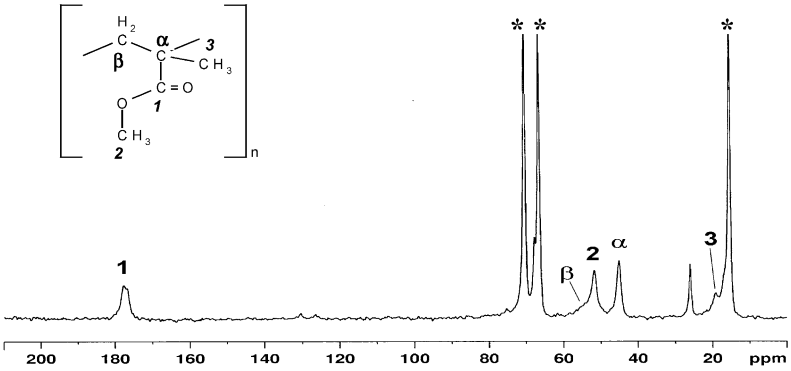


Fig. 7. $^{13}$C MAS NMR spectrum of membrane G2.

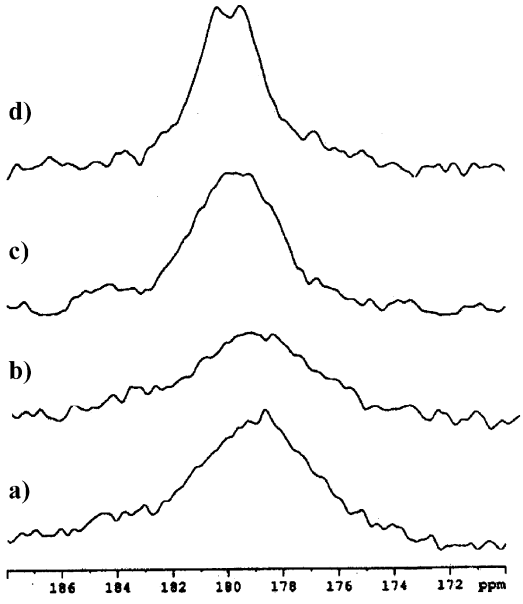


Fig. 8. Expansion of the low field region of the $^{13}C$ MAS NMR spectra of membranes Gn. (a) G2; (b) G3; (c) G4; (d) G5.

salt to have the maximum number of free charge carriers in the systems thus achieving best conductivity. For $[Li^+]=$ 0.8 M there is still some ester group mobility as justified by the weak bands in the 1270–1140 $cm^{-1}$ that almost disappear in the sample where the concentration of lithium perchlorate is 1 M. Such indication is supported by $^7Li$ spin–lattice relaxation times which show the highest value for $[Li^+]=0.8$ M.

Both spectroscopic data justify the highest conductivity value determined for G3.

## Acknowledgements

Thanks are due to Ms Cadia D'Ottavi for technical support. This work has been financed by ASI and MIUR.

## References

[1] Osaka Y, Kajiwara K, editors. Gels hanbook. San Diego, CA, USA: Academic Press; 2001.
[2] Hsu FY, Tsai SW, Wang FF, Wang YJ. Artif Cells, Blood Substitutes, Immobilization Biotechnol 2000;28:147–54.
[3] Hoffman AS. Adv Drug Delivery Rev 2002;43:3–12.
[4] Wang D, Williams CG, Li Q, Sharma B, Elisseeff JH. Biomaterials 2003;24:3969–80.
[5] Roy M, Gupta N. Chem Biol 2003;10:1161–71.
[6] Armand MB, Chabagno JM, Duclot M. In: Vashista P, Mundy JN, Shenoy GK, editors. Fast ion transport in solids. Amsterdam: Elsevier; 1979. p. 131.
[7] Scrosati B. Applications of electroactive polymers. London: Chapman & Hall; 1993.
[8] Gray FM, Armand MB. In: Besenhard JO, editor. Handbook of battery materials. Weinheim: Wiley; 1999.
[9] Song JY, Wang YY, Wan CC. J Power Sources 1999;77:183–97.
[10] Agnihotry SA, Nidhi G, Pradeep B, Sekon SS. Solid State Ionics 2000;573:136–7.
[11] Li Y, Yang MJ, Camaioni N, Casalbore-Miceli G. Sens Actuators B 2001;77:625–31.
[12] Iijima T, Toyoguchi Y, Eda N. Denki Kagaku 1985;53:619.
[13] Bohnke O, Rousselot C, Gillet PA, Truche C. J Electrochem Soc 1992;139:1862.
[14] Narici L, Bidoli V, Casolino M, De Pascale MP, Furano G, Modena I, et al. Adv Space Res 2003;31:141–6.
[15] Romagnoli P, Di Vona ML, Narici L, Sannita WG, Traversa E, Licoccia SJ. J Electrochem Soc 2001;148:63–6.
[16] Stallworth PE, Greenbaum SG, Croce F, Slane S, Salomon M. Electrochim Acta 1995;13-14:2137–41.
[17] Edmondson CA, Wintersgill MG, Fontanella JJ, Gerace F, Scrosati B, Greenbaum SG. Solid State Ionics 1996;85:173–9.
[18] Spěvaček J, Saiani A, Guenet JM. Macromol Rapid Commun 1996; 17:389.
[19] Buyse K, Berghmans H. Polymer 2000;41:1045–53.
[20] Van Den Broecke Ph, Berghmans H. Makromol Chem Macromol Symp 1990;39:59.
[21] Kusptov AH, Zhizhin GN. Handbook of Fourier transform Raman and infrared spectra of polymer. Amsterdam: Elsevier; 1998. p. 75.
[22] Chen H-W, Lin T-P, Chang F-C. Polymer 2002;43:5288–821.
[23] Dai Y, Wang Y, Greenbaum SG, Bajue SA, Golodnitsky D, Ardel G, et al. Electrochim Acta 1998;43:1557–61.